Volume 10 | Number 26 | 14 July 2019 | Pages 6395–6574

Chemical Science

rsc.li/chemical-science

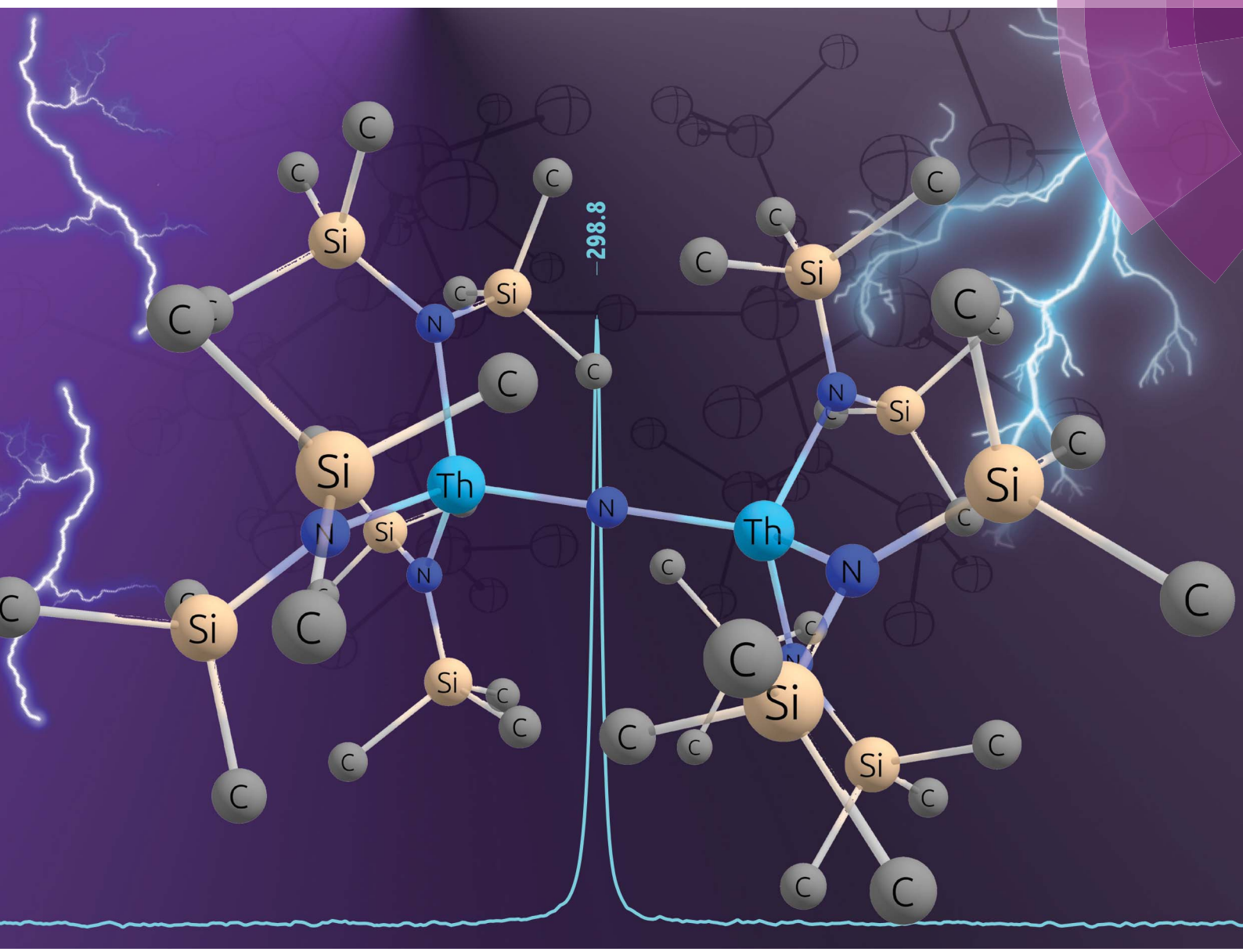

ISSN 2041-6539

ROYAL SOCIETY OF CHEMISTRY | Celebrating IYPT 2019

EDGE ARTICLE

Jochen Autschbach, Trevor W. Hayton *et al.*

Use of ^{15}N NMR spectroscopy to probe covalency in a thorium nitride

Chemical Science

EDGE ARTICLE

View Article Online
View Journal | View Issue

Cite this: *Chem. Sci.*, 2019, **10**, 6431

All publication charges for this article have been paid for by the Royal Society of Chemistry

Use of ^{15}N NMR spectroscopy to probe covalency in a thorium nitride†

Selena L. Staun,[a] Dumitru-Claudiu Sergentu,[b] Guang Wu,[a] Jochen Autschbach *[b] and Trevor W. Hayton *[a]

Received 19th April 2019
Accepted 2nd June 2019

DOI: 10.1039/c9sc01960j

rsc.li/chemical-science

Reaction of the thorium metallacycle, [Th{N(R)(SiMe$_2$)CH$_2$}(NR$_2$)$_2$] (R = SiMe$_3$) with 1 equiv. of NaNH$_2$ in THF, in the presence of 18-crown-6, results in formation of the bridged thorium nitride complex, [Na(18-crown-6)(Et$_2$O)][(R$_2$N)$_3$Th(μ-N)(Th(NR$_2$)$_3$] (**[Na][1]**), which can be isolated in 66% yield after work-up. Complex **[Na][1]** is the first isolable molecular thorium nitride complex. Mechanistic studies suggest that the first step of the reaction is deprotonation of [Th{N(R)(SiMe$_2$)CH$_2$}(NR$_2$)$_2$] by NaNH$_2$, which results in formation of the thorium bis(metallacycle) complex, [Na(THF)$_x$][Th{N(R)(SiMe$_2$CH$_2$)}$_2$(NR$_2$)], and NH$_3$. NH$_3$ then reacts with unreacted [Th{N(R)(SiMe$_2$)CH$_2$}(NR$_2$)$_2$], forming [Th(NR$_2$)$_3$(NH$_2$)] (**2**), which protonates [Na(THF)$_x$][Th{N(R)(SiMe$_2$CH$_2$)}$_2$(NR$_2$)] to give **[Na][1]**. Consistent with hypothesis, addition of excess NH$_3$ to a THF solution of [Th{N(R)(SiMe$_2$)CH$_2$}(NR$_2$)$_2$] results in formation of [Th(NR$_2$)$_3$(NH$_2$)] (**2**), which can be isolated in 51% yield after work-up. Furthermore, reaction of [K(DME)][Th{N(R)(SiMe$_2$CH$_2$)}$_2$(NR$_2$)] with **2**, in THF-d_8, results in clean formation of **[K][1]**, according to ^{1}H NMR spectroscopy. The electronic structures of **[1]**$^-$ and **2** were investigated by ^{15}N NMR spectroscopy and DFT calculations. This analysis reveals that the Th–N$_{nitride}$ bond in **[1]**$^-$ features more covalency and a greater degree of bond multiplicity than the Th–NH$_2$ bond in **2**. Similarly, our analysis indicates a greater degree of covalency in **[1]**$^-$ *vs.* comparable thorium imido and oxo complexes.

Introduction

The past decade has seen a remarkable expansion of the chemistry of actinide-ligand multiple bonds.[1–6] This is exemplified especially well by the chemistry of molecular uranium nitrides.[6] Since the synthesis of the first molecular uranium nitride in 2002,[7] many bridging and terminal uranium nitride complexes have been reported.[2,8–21] The study of these complexes has allowed actinide chemists to reveal fundamentally important insights into 5f covalency, as well as uncover novel modes of reactivity.[12,15–18,22–24]

In contrast, no isolable molecular thorium nitride complexes are known.[25] A handful of thorium nitrides have been identified in matrix isolation studies, such as ThN, NThN, and NThO, but these are only stable at cryogenic temperatures.[26–28] Recently, Liddle and co-workers reported the isolation of the bridged Th(IV) parent imido complex, [{Th(Tren^{DMBS})}$_2$(μ-NH)] (Tren^{DMBS} = {N(CH$_2$CH$_2$NSiMe$_2$^{t}Bu)$_3$}$^{3-}$), which was thought to form *via* an unobserved Th nitride intermediate, [{Th(Tren^{DMBS})}$_2$(μ-N)]$^-$.[25] It was postulated that the nitride ligand in this intermediate was exceptionally basic on account of its highly polarized Th–N$_{nitride}$ bonds. As a result, it spontaneously deprotonated the solvent, forming the bridged parent imido. These results prompted the authors of ref. 25 to suggest that the Th=N=Th unit may be intrinsically more reactive than the more covalent U=N=U unit. Significantly, further work in this area would allow us to evaluate this hypothesis in more detail, as well as permit a better evaluation of the bonding within this functional group.

Herein, we report the synthesis of the first isolable molecular thorium nitride complex, [Na(18-crown-6)(Et$_2$O)][(R$_2$N)$_3$Th(μ-N)Th(NR$_2$)$_3$] (R = SiMe$_3$). In addition, we report its characterization by ^{15}N NMR spectroscopy and DFT calculations, which has allowed us to evaluate the degree of 5f covalency within the Th=N=Th unit. To provide context, we have synthesized the parent amide complex, [Th(NR$_2$)$_3$(NH$_2$)]. This material was also characterized by ^{15}N NMR spectroscopy and density functional theory (DFT) calculations.

Synthesis and characterization

Addition of 1 equiv. of NaNH$_2$ to a cold (−25 °C) solution of the thorium metallacycle,[29] [Th{N(R)(SiMe$_2$)CH$_2$}(NR$_2$)$_2$] (R =

[a]*Department of Chemistry and Biochemistry, University of California, Santa Barbara, California 93106, USA. E-mail: hayton@chem.ucsb.edu*

[b]*Department of Chemistry, University at Buffalo, State University of New York, 312 Natural Sciences Complex, Buffalo, NY 14260-3000, USA. E-mail: jochena@buffalo.edu*

† Electronic supplementary information (ESI) available: Experimental procedures, crystallographic details (as CIF files), computational results, and spectral data for complexes **[Na][1]**, **[K][1]**, **2**, **[K][1-^{15}N]**, and **2-^{15}N**. CCDC 1911146–1911148. For ESI and crystallographic data in CIF or other electronic format see DOI: 10.1039/c9sc01960j

$SiMe_3$), in tetrahydrofuran (THF), followed by addition of 1 equiv. of 18-crown-6, afforded the bridged nitride complex, $[Na(18\text{-crown-6})(Et_2O)][(R_2N)_3Th(\mu\text{-}N)(Th(NR_2)_3]$ (**[Na][1]**), after stirring for 24 h. This material could be isolated as colorless plates in 66% yield after work-up (eqn (1)). The reaction of $[Th\{N(R)(SiMe_2)CH_2\}(NR_2)_2]$ with 0.5 equiv. of both $NaNH_2$ and 18-crown-6 also generates **[Na][1]**, but with reduced yields (30%). The isolation of **[Na][1]** contrasts with the recent results of Liddle and co-workers, who attempted to isolate a bridged thorium nitride complex by reduction of a Th azide precursor, but isolated the bridged parent imido complex, $[\{Th(Tren^{DMBS})\}_2(\mu\text{-}NH)]$, instead.[25]

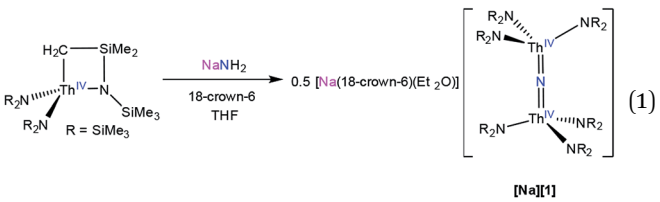

(1)

The connectivity of complex **[Na][1]** was verified by X-ray crystallography (Fig. 1; see ESI† for complete structural details). Complex **[Na][1]** crystallizes in the monoclinic space group $P2_1/c$. In the solid-state, each Th center features a pseudo-tetrahedral coordination geometry. In addition, the Th–$N_{nitride}$–Th linkage is linear (179(1)°), while its Th–$N_{nitride}$ bond lengths (Th1–N1 = 2.14(2), Th2–N1 = 2.11(2) Å) are much shorter than the Th–$N_{silylamido}$ bond lengths (av. 2.41 Å), suggesting multiple-bond character in the former. A $[Na(18\text{-crown-6})(Et_2O)]^+$ counterion is also present in the unit cell. The potassium analog, $[K(18\text{-crown-6})(THF)_2][(R_2N)_3Th(\mu\text{-}N)Th(NR_2)_3]$ (**[K][1]**), has also been structurally characterized. It features nearly identical metrical parameters to those of **[Na][1]** (See ESI† for full details).

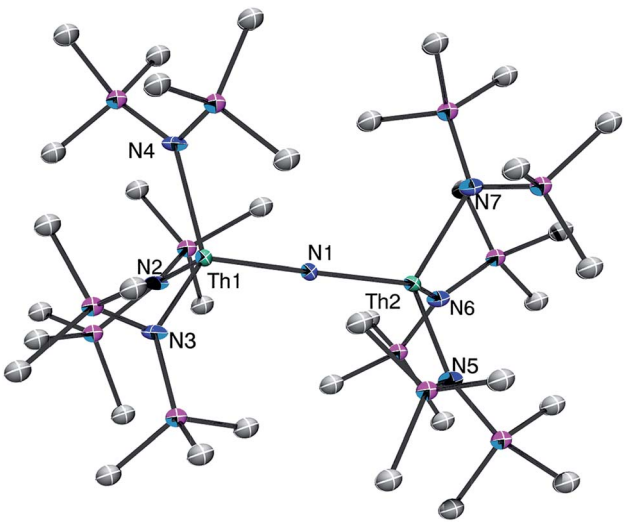

Fig. 1 Solid-state molecular structure of **[Na][1]**, shown with 50% probability ellipsoids. Hydrogen atoms and $[Na(18\text{-crown-6})(Et_2O)]^+$ counterion removed for clarity. Selected bond lengths (Å) and angles (°): Th1–N1 = 2.14(2), Th2–N1 = 2.11(2), Th1–N1–Th2 = 179(1), av. Th1–N_{amido} = 2.41, av. Th2–N_{amido} = 2.41, av. N_{amido}–Th1–N_{amido} = 108.3, av. N_{amido}–Th2–N_{amido} = 108.7.

Complex **[Na][1]** is the first nitrido complex reported for thorium. However, several thorium imido complexes have been structurally characterized.[30–36] Generally, these complexes feature shorter Th–N bonds than those of **[Na][1]**. For example, $[Cp_2^*Th(N\text{-}2,6\text{-}Me_2C_6H_3)(THF)]$ features a Th–N distance of 2.045(8) Å,[32] and $[K(18\text{-crown-6})][Th(=NDipp)(NR_2)_3]$ (Dipp = 2,6-$^iPr_2C_6H_3$) features a Th–N distance of 2.072(3) Å.[30] For further comparison, the bridged U(IV) nitride, $[Na][(\mu\text{-}N)(U(N[t\text{-}Bu]Ar)_3)_2]$ (Ar = 3,5-$Me_2C_6H_3$), also features a linear U=N=U linkage (175.1(2)°), but shorter An–N bond distances (2.080(4) Å and 2.077(4) Å),[11] consistent with the smaller ionic radius of uranium. Similar metric parameters are observed in $[Cs][\{U(OSi(O^tBu)_3)_3\}_2(\mu\text{-}N)]$ (U–N–U = 170.2(3)°; U1–N1 = 2.058(5) Å; U2–N1 = 2.079(5) Å).[12]

The ^{1}H NMR spectrum of **[Na][1]** in THF-d_8 features a sharp singlet at 0.36 ppm, assignable to the $SiMe_3$ groups, along with a broad resonance at 3.62 ppm, assignable to the 18-crown-6 moiety. Complex **[Na][1]** is insoluble in pentane and benzene, but is quite soluble in Et_2O and THF. It is stable as a THF-d_8 solution at room temperature for at least 24 h, showing minimal signs of decomposition over this time. Finally, the IR spectrum of **[Na][1]** features a mode at 742 cm^{-1}, which corresponds to the principal Th–N–Th asymmetric stretch (Fig. S15†). For comparison, this mode was calculated to occur at 758 cm^{-1} (Fig. S30, see ESI† for calculation details).

To better understand the mechanism of formation of **[Na][1]** we monitored the reaction of $[Th\{N(R)(SiMe_2)CH_2\}(NR_2)_2]$ with $NaNH_2$ and 18-crown-6, in THF-d_8, by ^{1}H NMR spectroscopy (Fig. S12†). A ^{1}H NMR spectrum of this mixture after 7 h revealed an intense new resonance at 0.36 ppm, which is assignable to **[Na][1]**. Interestingly, this spectrum also features minor resonances at 0.30 and 0.18 ppm, which are assignable to the terminal parent amide complex, $[Th(NR_2)_3(NH_2)]$ (**2**), and the bis(metallacycle) complex, $[Na(THF)_x][Th\{N(R)(SiMe_2CH_2)\}_2(NR_2)]$,[30] respectively. The assignment for the latter species was made by comparison with the ^{1}H NMR spectrum of the known bis(metallacycle) complex, $[K(DME)][Th\{N(R)(SiMe_2CH_2)\}_2(NR_2)]$.[30] After 32 h, the resonance assignable to **[Na][1]** has grown in intensity, while the resonances assignable to $[Th\{N(R)(SiMe_2)CH_2\}(NR_2)_2]$ and **2** have completely disappeared, and only trace amounts of $[Na(THF)_x][Th\{N(R)(SiMe_2CH_2)\}_2(NR_2)]$ are still present in solution. To explain these observations, we suggest that the first step of the reaction is deprotonation of $[Th\{N(R)(SiMe_2)CH_2\}(NR_2)_2]$ by $NaNH_2$, forming $[Na(THF)_x][Th\{N(R)(SiMe_2CH_2)\}_2(NR_2)]$ and NH_3 (Scheme 1). NH_3 then reacts with unreacted $[Th\{N(R)(SiMe_2)CH_2\}(NR_2)_2]$, forming **2**, which then protonates $[Na(THF)_x][Th\{N(R)(SiMe_2CH_2)\}_2(NR_2)]$ to give **[Na][1]**.

To test this hypothesis we explored the reaction of $[Th\{N(R)(SiMe_2)CH_2\}(NR_2)_2]$ with NH_3. Thus, addition of 3 equiv. of NH_3, as a 0.4 M solution in THF, to a THF solution of $[Th\{N(R)(SiMe_2)CH_2\}(NR_2)_2]$ results in rapid formation of **2**, which can be isolated in 51% yield after work-up (eqn (2)).

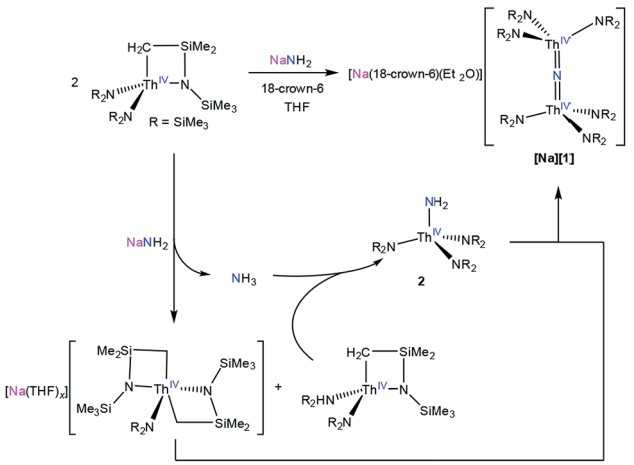

Scheme 1 Proposed mechanism of formation of [Na][1].

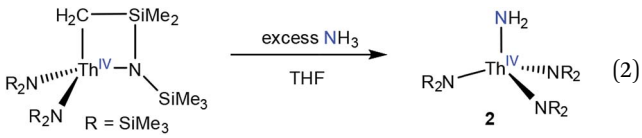

(2)

The ^{1}H NMR spectrum of **2** in C_6D_6 features a sharp resonance at 0.37 ppm (54H), assigned to the $SiMe_3$ groups. In addition, a 1 : 1 : 1 triplet (2H, J_{NH} = 45.8 Hz) at 3.67 ppm is assigned to the –NH_2 resonance (Fig. S5†). For comparison, the J_{NH} values for the isostructural group(IV) complexes, $[M(NR_2)_3(NH_2)]$ (M = Zr, Hf), were found to be 45.6 Hz (Zr) and 46.0 Hz (Hf).[37] Interestingly, the only other known thorium NH_2 complex, $[K(DME)_4][(DME)Th(NH_2)(diphenolate)_2]$, featured a broad singlet at 2.0 ppm in its ^{1}H NMR spectrum, which was assignable to the –NH_2 group.[38]

The connectivity of complex **2** was verified by X-ray crystallography (Fig. 2, see ESI† for complete structural details).

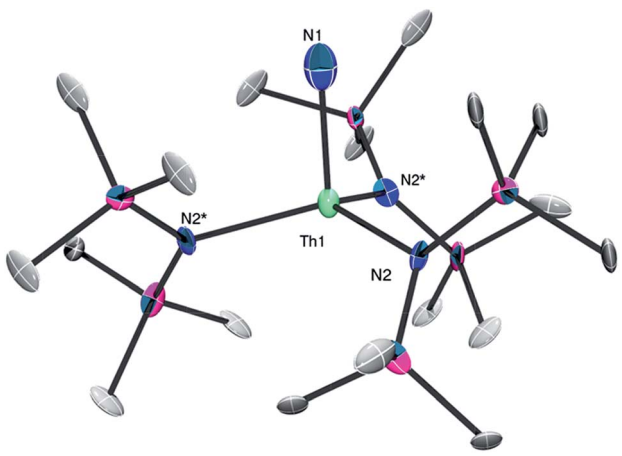

Fig. 2 Solid-state molecular structure of **2**, shown with 50% probability ellipsoids. Hydrogen atoms removed for clarity. Selected bond lengths (Å) and angles (°): Th1–N1 = 2.24(6), Th1–N2 = 2.36(2), N1–Th1–N2 = 100.7(3), N2–Th1–N2* = 116.7(2).

Complex **2** crystallizes in the trigonal space group $R\bar{3}c$. In the solid-state, complex **2** is disordered over two positions in a 50 : 50 ratio, which somewhat lowers the precision of the resulting metrical parameters. It features a pseudo-tetrahedral geometry about the thorium center. Due to the large ESDs, the Th–NH_2 distance (2.24(6) Å) in **2** is statistically identical to its Th–$N_{silylamido}$ distances (2.36(2) Å).[30,39] The other Th–NH_2 complex has a similar Th–NH_2 bond length (2.2431(6) Å).[38] For further comparison, the uranium(IV) terminal amide complexes, $[U(NH_2)(Tren^{TIPS})]$ ($Tren^{TIPS}$ = $\{N(CH_2CH_2NSi^iPr_3)_3\}^{3-}$) and $[\{\eta^5$-1,2,4-$C_5H_2{}^tBu_3\}_2U(NH_2)_2]$, feature U–$NH_2$ bond lengths of 2.228(4) and 2.19 Å (av.), respectively.[40,41]

Complex **2** is highly soluble in pentane, benzene, Et_2O and THF. Furthermore, **2** is stable as a C_6D_6 solution for over 36 h with minimal signs of decomposition. In addition, the IR spectrum of **2** features a prominent N–H stretching mode at 3321 cm^{-1} (Fig. S21, ESI†), providing further support for our formulation. For comparison, this mode is observed at 3342 cm^{-1} (Zr) and 3364 cm^{-1} (Hf) for $[M(NR_2)_3(NH_2)]$ (M = Zr, Hf).[37]

To further test our proposed mechanistic hypothesis, we monitored the reaction of $[K(DME)][Th\{N(R)(SiMe_2CH_2)\}_2(NR_2)]$[30] with **2** in THF-$d_8$, in the presence of 1 equiv. of 18-crown-6, by ^{1}H NMR spectroscopy (eqn (3)). A ^{1}H NMR spectrum of this solution, after standing at room temperature for 4 h, reveals a new resonance at 0.36 ppm, which is assignable to **[K][1]** (Fig. S13†). After 3d, the peak assignable to the nitride has increased in intensity, while resonances assignable to complex **2** and $[K(DME)][Th\{N(R)(SiMe_2CH_2)\}_2(NR_2)]$ have decreased in intensity. These three complexes are present in a ratio of 1 : 3 : 6.7 in the 3d spectrum. Overall, this result supports the proposed mechanism (Scheme 1), but it is important to note that formation of $[\mathbf{1}]^-$ under these conditions is much slower than its rate of formation under the conditions described in eqn (1), suggesting that this experiment does not perfectly duplicate the original reaction conditions.

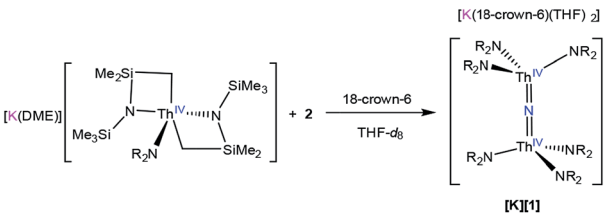

(3)

To facilitate our covalency analysis we endeavoured to synthesize $[\mathbf{1}\text{-}^{15}\mathbf{N}]^-$. Given the proposed intermediacy of $[Na(THF)_x][Th\{N(R)(SiMe_2CH_2)\}_2(NR_2)]$ in the formation of **[Na][1]**, we rationalized that reaction of NH_4Cl with 2 equiv. of $[Th\{N(R)(SiMe_2CH_2)\}_2(NR_2)]^-$ would generate the nitride complex. Thus, addition of 1 equiv. of finely ground $^{15}NH_4Cl$ to a pale yellow THF solution containing 2 equiv. of $[K(DME)][Th\{N(R)(SiMe_2CH_2)\}_2(NR_2)]$,[30] followed by addition of 1 equiv. of 18-crown-6, results in formation of $[K(18\text{-crown-6})(THF)_2][(R_2N)_3Th(\mu\text{-}^{15}N)(Th(NR_2)_3]$ (**[K][1-^{15}N]**), which can be isolated as a white powder in 13% yield after work-up (eqn (4)).

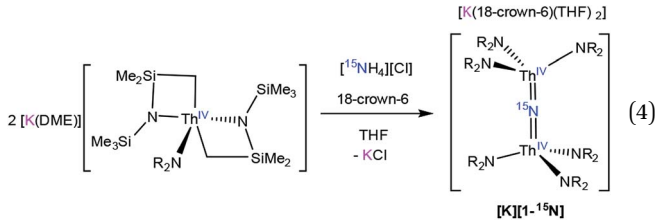

(4)

The low yield of **[K][1-^{15}N]** under these conditions can be partly ascribed to unselective protonation of [K(DME)][Th{N(R)(SiMe$_2$CH$_2$)}$_2$(NR$_2$)] by ^{15}NH$_4$Cl, which results in the formation of copious amounts of HNR$_2$ (observed in the *in situ* ^{1}H NMR spectrum), and results in the presence of unreacted [K(DME)][Th{N(R)(SiMe$_2$CH$_2$)}$_2$(NR$_2$)] in the final reaction mixture. The unreacted [K(DME)][Th{N(R)(SiMe$_2$CH$_2$)}$_2$(NR$_2$)] can be conveniently removed from the nitride product by rinsing with toluene. The ^{1}H NMR spectrum of **[K][1-^{15}N]** in THF-d_8 matches those recorded for both **[Na][1]** and **[K][1]** (see ESI† for full details), where a singlet at 0.36 ppm can be assigned to the SiMe$_3$ groups and a resonance at 3.63 ppm can be assigned to 18-crown-6. Furthermore, the ^{15}N{^{1}H} NMR spectrum of **[K][1-^{15}N]** (referenced to CH$_3$NO$_2$) reveals a sharp singlet at 298.8 ppm. No other resonances are observed in this spectrum. This is the first observation of an ^{15}N chemical shift for an actinide nitride. For comparison, the group 4 nitride complexes [{(η^5-C$_5$H$_2$-1,2,4-Me$_3$)$_2$Hf}$_2$(μ-N)(NCO)(DMAP)] and [{Cp*TiCl$_2$}(μ-N){Cp*TiCl(NH$_3$)}] feature ^{15}N resonances at 567.19 ppm and 431.6 ppm, respectively, for their bridging nitride ligands.[42,43] Finally, the IR spectrum of **[K][1-^{15}N]** features a stretch at 735 cm^{-1}, which corresponds to the principal Th–N–Th asymmetric stretch (Fig. S17†), and is redshifted by 7 cm^{-1} from that observed for **[Na][1]**.

Finally, access to **2-^{15}N** was achieved by reaction of [Th{N(R)(SiMe$_2$)CH$_2$}(NR$_2$)$_2$] with 1 equiv. of ^{15}NH$_3$ gas in THF. Synthesized in this manner, colorless crystals of **2-^{15}N** could be isolated in 85% yield after work-up. Similar to **2**, the ^{1}H NMR spectrum in benzene-d_6 shows a singlet at 0.36 ppm (54H), assignable to the SiMe$_3$ groups. In addition, a 1 : 1 doublet (2H, J_{NH} = 62.3 Hz) at 3.67 ppm is assignable to the –NH$_2$ resonance (Fig. S9, ESI†). The ^{15}N NMR spectrum of **2-^{15}N** (referenced to CH$_3$NO$_2$) reveals a sharp resonance at −198.4 ppm. For comparison, the previously reported thorium amide ^{15}N NMR spectrum featured a sharp triplet centered at 155.01 ppm (J = 57.2 Hz).[38] It is not readily apparent why this chemical shift is so different from that recorded for complex **2-^{15}N**. Finally, the IR spectrum of **2-^{15}N** features an N–H stretch at 3317 cm^{-1}, and a Th–NH$_2$ stretch at 482 cm^{-1} (Fig. S22, ESI†). The identity of the latter stretch was confirmed by comparison with the calculated IR spectrum (Fig. S31†), where it is predicted to occur at 508 cm^{-1}.

Electronic structure analysis

We analyzed the electronic structures of **[1]**$^-$ and **2** with DFT. Using the B3LYP functional, we observe excellent agreement between the calculated and experimentally determined structural parameters for both complexes. For example, the calculated Th–N$_{nitride}$ and Th–N$_{silylamide}$ bond lengths for **[1]**$^-$ are within 0.02 Å of the distances found in the solid state. Similarly, the calculated Th–N$_{amide}$ and Th–N$_{silylamide}$ bond lengths in **2** are within 0.02 Å of those found in its crystal structure.

An NBO/NLMO analysis of **[1]**$^-$ reveals that the Th–N–Th interaction consists of two orthogonal 3c–2e π bonds and two predominantly 2c–2e σ bonds that feature some three-center character (Fig. 3), suggestive of overall Th=N double bond character. The covalency in the Th–N$_{nitride}$ bonds in **[1]**$^-$ is greater than that observed for the related Th imido, [Th(NAr)(NR$_2$)$_3$]$^-$ (Ar = 2,6-^{i}Pr$_2$C$_6$H$_3$),[30] and Th oxo, [Th(O)(NR$_2$)$_3$]$^-$,[44] with a greater magnitude of 5f orbital involvement. For example, the Th–N π interaction in **[1]**$^-$ features 16% Th character (58% 6d, 42% 5f) (Table 1), whereas [Th(NAr)(NR$_2$)$_3$]$^-$ and [Th(O)(NR$_2$)$_3$]$^-$ feature 0% and 12% Th character (65% 6d, 35% 5f), respectively, in their Th–E π bonds. For further comparison, the degree of covalency in **[1]**$^-$ is comparable to that observed for the thorium sulfide, [Th(S)(NR$_2$)$_3$]$^-$, which features 17% Th character (61% 6d, 38% 5f) in its Th–S π interaction.[44] The Wiberg bond index of the Th–N$_{nitride}$ bond is 0.94, which is greater than that calculated for [Th(NAr)(NR$_2$)$_3$]$^-$ (0.88).[30] Overall, these combined computational metrics indicate a greater degree of covalency in **[1]**$^-$ *vs.* the comparable imido and oxo complexes. Similar observations have been made for uranium(v) nitride and oxo complexes.[21,40,45]

For complex **2**, an NBO/NLMO analysis reveals that the Th–N interaction consists of 2c–2e π bond and a 2c–2e σ bond (Fig. S28†). Not surprisingly, the degree of covalency within the Th–N$_{amide}$ bond in **2** is less than that observed for the Th=N= Th bonds of **[1]**$^-$. Specifically, the σ bond in **2** features 7% Th character (63% 6d, 21% 5f, 5% 7p, 11% 7s) and the π bond features 10% Th character (59% 6d, 41% 5f). Accordingly, the

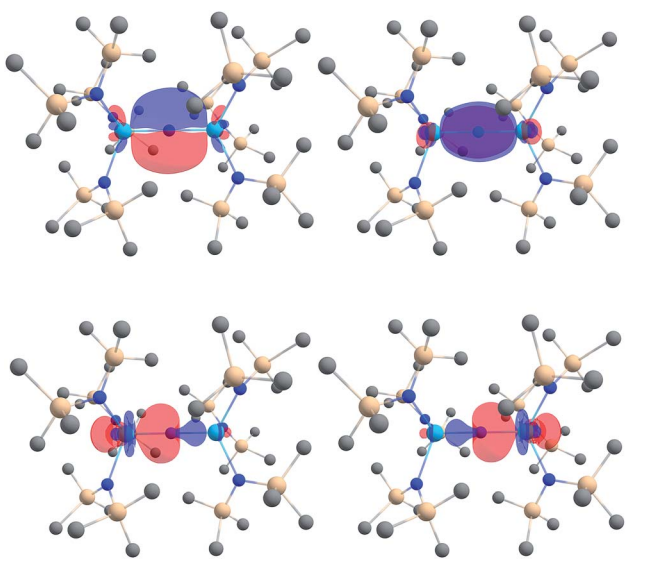

Fig. 3 Th–N (2σ + 2π) bonding NLMOs in [(NR$_2$)$_3$Th(μ-N)Th(NR$_2$)$_3$]$^-$ (isosurface plots ±0.03 au; hydrogen atoms are omitted for clarity). Color code for atoms: Th, light blue; N, blue; Si, beige; C, gray.

Table 1 % compositions of the Th–N bonding NLMOs in $[(NR_2)_3Th(\mu\text{-}N)Th(NR_2)_3]^-$

	% N			% Th				
Orbital	Total N	2s	2p	Total Th	7s	7p	6d	5f
σ	87	51	49	10	3	6	67	24
				3[a]	2	10	30	58
π	84	0	100	16	0	0	58	42

[a] The σ-bonding orbitals have some three-center character, each with 10 *vs.* 3% weight from the two Th centers.

Wiberg bond index of the $Th–N_{amide}$ bond (0.65) is substantially less than that observed for the $Th–N_{nitride}$ bonds in **[1]**$^-$.

Chemical shift analysis

To assess the accuracy of our computational approach, we calculated the ^{15}N chemical shift of the nitride ligand in the known group(IV) nitride complex, $[\{Cp^*TiCl_2\}(\mu\text{-}N)\{Cp^*TiCl(NH_3)\}]$.[42] The ^{15}N chemical shift of the nitride ligand for the B3LYP-optimized structure was calculated to be 406.8/421.8 ppm using the PBE0/B3LYP functionals and the scalar relativistic (SR) all-electron ZORA Hamiltonian. For comparison, the experimentally determined chemical shift is 431.6 ppm.[42] Even better agreement was achieved by performing the calculation with two-component ZORA, *i.e.*, including the spin–orbit (SO) coupling variationally. At this level, the calculated chemical shift (414.5/430.5 ppm) is in very good agreement with experiment.

With these results in hand, the ^{15}N NMR chemical shifts for the nitride and NH_2 ligands in **[1]**$^-$ and **2** were calculated using the PBE0 functional. We, and others, have found that this functional typically works better than B3LYP for NMR shift calculations in actinide-containing molecules.[46] For **[1]**$^-$, the calculated ^{15}N chemical shift without spin orbit coupling (ZORA-SR) is 226 ppm – substantially upfield from the experimental result (298.8 ppm). Considerably better agreement is obtained when SO coupling is taken into account, with a calculated ^{15}N shift of 305 ppm. The 79 ppm downfield shift induced by SO coupling is evidence of 5f (and 6d) character in the $Th–N_{nitride}$ bonds. For **2**, the calculated ^{15}N chemical shift without SO coupling is −254 ppm. Upon inclusion of SO coupling, the shift changes to −210 ppm, which is much closer to the measured value (−198.4 ppm). The smaller downfield shift induced by SO coupling in **2** ($\Delta\delta$ = 44 ppm) is consistent with the reduced covalency, and reduced bond multiplicity, of the $Th–N_{amide}$ bond. Perhaps most importantly, the good agreement between the experimental and calculated shifts for both **[1]**$^-$ and **2** gives credence to the NBO analysis presented above.

Conclusions

We have synthesized and characterized the first isolable molecular thorium nitride complex, $[(NR_2)_3Th(\mu\text{-}N)Th(NR_2)_3]^-$. This complex is thermally stable, in contrast to the bridged thorium nitride recently proposed by Liddle and co-workers.[25] The origin of this stability difference is not known, but it may be related to the lack of a *trans* donor ligand in $[(NR_2)_3Th(\mu\text{-}N)Th(NR_2)_3]^-$ *vs.* $[\{Th(Tren^{DMBS})\}_2(\mu\text{-}N)]^-$. Alternatively, it could relate to the different method of synthesis. ^{15}N NMR spectroscopic characterization of $[(NR_2)_3Th(\mu\text{-}N)Th(NR_2)_3]^-$, in combination with a DFT analysis, reveals the presence of 5f orbital participation within the Th=N=Th unit. In line with the reduced electronegativity of nitrogen *vs.* oxygen, our data suggests greater levels of covalency in $[(NR_2)_3Th(\mu\text{-}N)Th(NR_2)_3]^-$ than in the closely related oxo, $[Th(O)(NR_2)_3]^-$. However, we find comparable covalency in $[(NR_2)_3Th(\mu\text{-}N)Th(NR_2)_3]^-$ to that found in the thorium sulfide, $[Th(S)(NR_2)_3]^-$, likely on account of the greater "energy-driven" overlap in the latter.[47] To better contextualize our results, we also synthesized and characterized the thorium parent amide complex, $[Th(NR_2)_3(NH_2)]$. According to ^{15}N NMR spectroscopy and DFT calculations, this complex features a lesser degree of 5f covalency in its $Th–NH_2$ bond than that found for the bridging nitride complex, which is not surprising given its reduced bond order.

This work further solidifies the use of NMR spectroscopy as an important tool for probing the electronic structure of the actinides. Previously, ^{13}C, ^{77}Se, and ^{125}Te NMR spectroscopies had been used to evaluate covalency in An–E bonds.[39,46,48–51] In the case of An–C bonding, large downfield ^{13}C shifts have been consistently observed for the ^{13}C nuclei bonded directly to an actinide center. More significantly, the degree of deshielding was found to correlate with the amount of 5f covalency within the An–C bond. For example, the ^{13}C NMR shift of acetylide carbon in the U(VI) acetylide complexes, $U^{VI}(O)(C{\equiv}CC_6H_4\text{-}p\text{-}R)(NR_2)_3$ (R = NMe_2, OMe, Me, Ph, H, Cl), correlated well with two measures of covalency, the QTAIM delocalization index and the Wiberg bond order of the U–C bond.[48] Highly deshielded ^{13}C resonances are also observed for the carbene resonance in $[Th(CHPPh_3)(NR_2)_3]$ and the methylene resonances in $[UO_2(\text{-}CH_2SiMe_3)_4]^{2-}$ and $[U(CH_2SiMe_3)_6]^-$.[46,52] Our results demonstrate that ^{15}N NMR spectroscopy can also be used to evaluate covalency in actinide-ligand bonding, and like ^{13}C NMR spectroscopy, the magnitude of the downfield shift correlates with the degree of 5f character in the An–N bond. Going forward, we propose to characterize other actinide nitrides by ^{15}N NMR spectroscopy. Of particular interest is the measurement of the ^{15}N chemical shift of a U(VI) nitride complex, which, on account of the high anticipated covalency, should exhibit an extreme downfield shift of its nitride resonance.

Conflicts of interest

There are no conflicts to declare.

Acknowledgements

This work was supported by the U.S. Department of Energy, Office of Basic Energy Sciences, Chemical Sciences, Biosciences, and Geosciences Division, under Contract DE-SC0001861. D. C. S. and J. A. acknowledge support from the U.S. Department of Energy, Office of Basic Energy Sciences, Heavy Element Chemistry program under grant DE-SC0001136 and the UB Center for

Computational Research (CCR) for the computational part of this study. The authors thank the Ménard group (UCSB) for the use of their $^{15}NH_3$.

Notes and references

1 T. W. Hayton, *Dalton Trans.*, 2010, **39**, 1145–1158.
2 T. W. Hayton, *Chem. Commun.*, 2013, **49**, 2956–2973.
3 M. B. Jones and A. J. Gaunt, *Chem. Rev.*, 2013, **113**, 1137–1198.
4 D. Patel and S. T. Liddle, *Prog. Inorg. Chem.*, 2012, **32**, 1.
5 S. T. Liddle, *Angew. Chem., Int. Ed.*, 2015, **54**, 8604–8641.
6 D. M. King and S. T. Liddle, *Coord. Chem. Rev.*, 2014, **266–267**, 2–15.
7 I. Korobkov, S. Gambarotta and G. P. A. Yap, *Angew. Chem., Int. Ed.*, 2002, **41**, 3433–3436.
8 W. J. Evans, S. A. Kozimor and J. W. Ziller, *Science*, 2005, **309**, 1835.
9 M. Falcone, L. Chatelain, R. Scopelliti, I. Živković and M. Mazzanti, *Nature*, 2017, **547**, 332.
10 S. Fortier, G. Wu and T. W. Hayton, *J. Am. Chem. Soc.*, 2010, **132**, 6888–6889.
11 A. R. Fox, P. L. Arnold and C. C. Cummins, *J. Am. Chem. Soc.*, 2010, **132**, 3250–3251.
12 L. Chatelain, R. Scopelliti and M. Mazzanti, *J. Am. Chem. Soc.*, 2016, **138**, 1784–1787.
13 P. A. Cleaves, C. E. Kefalidis, B. M. Gardner, F. Tuna, E. J. L. McInnes, W. Lewis, L. Maron and S. T. Liddle, *Chem.–Eur. J.*, 2017, **23**, 2950–2959.
14 P. A. Cleaves, D. M. King, C. E. Kefalidis, L. Maron, F. Tuna, E. J. L. McInnes, J. McMaster, W. Lewis, A. J. Blake and S. T. Liddle, *Angew. Chem., Int. Ed.*, 2014, **53**, 10412–10415.
15 M. Falcone, L. Chatelain and M. Mazzanti, *Angew. Chem., Int. Ed.*, 2016, **55**, 4074–4078.
16 M. Falcone, L. Chatelain, R. Scopelliti and M. Mazzanti, *Chimia*, 2017, **71**, 209–212.
17 M. Falcone, C. E. Kefalidis, R. Scopelliti, L. Maron and M. Mazzanti, *Angew. Chem., Int. Ed.*, 2016, **55**, 12290–12294.
18 M. Falcone, L. N. Poon, F. Fadaei Tirani and M. Mazzanti, *Angew. Chem., Int. Ed.*, 2018, **57**, 3697–3700.
19 T. W. Hayton, *Nat. Chem.*, 2013, **5**, 451.
20 D. M. King, P. A. Cleaves, A. J. Wooles, B. M. Gardner, N. F. Chilton, F. Tuna, W. Lewis, E. J. L. McInnes and S. T. Liddle, *Nat. Commun.*, 2016, **7**, 13773.
21 D. M. King, F. Tuna, E. J. L. McInnes, J. McMaster, W. Lewis, A. J. Blake and S. T. Liddle, *Science*, 2012, **337**, 717.
22 K. C. Mullane, H. Ryu, T. Cheisson, L. N. Grant, J. Y. Park, B. C. Manor, P. J. Carroll, M.-H. Baik, D. J. Mindiola and E. J. Schelter, *J. Am. Chem. Soc.*, 2018, **140**, 11335–11340.
23 R. K. Thomson, T. Cantat, B. L. Scott, D. E. Morris, E. R. Batista and J. L. Kiplinger, *Nat. Chem.*, 2010, **2**, 723.
24 M. Falcone, L. Barluzzi, J. Andrez, F. Fadaei Tirani, I. Zivkovic, A. Fabrizio, C. Corminboeuf, K. Severin and M. Mazzanti, *Nat. Chem.*, 2019, **11**, 154–160.
25 J. Du, D. M. King, L. Chatelain, E. Lu, F. Tuna, E. J. L. McInnes, A. J. Wooles, L. Maron and S. T. Liddle, *Chem. Sci.*, 2019, **10**, 3738–3745.
26 D. W. Green and G. T. Reedy, *J. Mol. Spectrosc.*, 1979, **74**, 423–434.
27 G. P. Kushto, P. F. Souter and L. Andrews, *J. Chem. Phys.*, 1998, **108**, 7121–7130.
28 B. Vlaisavljevich, L. Andrews, X. Wang, Y. Gong, G. P. Kushto and B. E. Bursten, *J. Am. Chem. Soc.*, 2016, **138**, 893–905.
29 T. Cantat, B. L. Scott and J. L. Kiplinger, *Chem. Commun.*, 2010, **46**, 919–921.
30 N. L. Bell, L. Maron and P. L. Arnold, *J. Am. Chem. Soc.*, 2015, **137**, 10492–10495.
31 M. E. Garner, S. Hohloch, L. Maron and J. Arnold, *Organometallics*, 2016, **35**, 2915–2922.
32 A. Haskel, T. Straub and M. S. Eisen, *Organometallics*, 1996, **15**, 3773–3775.
33 W. Ren, G. Zi and M. D. Walter, *Organometallics*, 2012, **31**, 672–679.
34 T. Straub, A. Haskel, T. G. Neyroud, M. Kapon, M. Botoshansky and M. S. Eisen, *Organometallics*, 2001, **20**, 5017–5035.
35 P. Yang, E. Zhou, G. Hou, G. Zi, W. Ding and M. D. Walter, *Chem.–Eur. J.*, 2016, **22**, 13845–13849.
36 C. Zhang, P. Yang, E. Zhou, X. Deng, G. Zi and M. D. Walter, *Organometallics*, 2017, **36**, 4525–4538.
37 X. Yu and Z.-L. Xue, *Inorg. Chem.*, 2005, **44**, 1505–1510.
38 I. Korobkov, S. Gambarotta and G. P. A. Yap, *Angew. Chem., Int. Ed.*, 2003, **42**, 4958–4961.
39 D. E. Smiles, G. Wu, P. Hrobárik and T. W. Hayton, *J. Am. Chem. Soc.*, 2016, **138**, 814–825.
40 D. M. King, F. Tuna, E. J. L. McInnes, J. McMaster, W. Lewis, A. J. Blake and S. T. Liddle, *Nat. Chem.*, 2013, **5**, 482.
41 G. Zi, L. Jia, E. L. Werkema, M. D. Walter, J. P. Gottfriedsen and R. A. Andersen, *Organometallics*, 2005, **24**, 4251–4264.
42 A. Abarca, P. Gómez-Sal, A. Martín, M. Mena, J. M. Poblet and C. Yélamos, *Inorg. Chem.*, 2000, **39**, 642–651.
43 S. P. Semproni, C. Milsmann and P. J. Chirik, *Angew. Chem.*, 2012, **51**, 5213–5216.
44 D. E. Smiles, G. Wu, N. Kaltsoyannis and T. W. Hayton, *Chem. Sci.*, 2015, **6**, 3891–3899.
45 D. M. King, F. Tuna, J. McMaster, W. Lewis, A. J. Blake, E. J. L. McInnes and S. T. Liddle, *Angew. Chem., Int. Ed.*, 2013, **52**, 4921–4924.
46 D. E. Smiles, G. Wu, P. Hrobárik and T. W. Hayton, *Organometallics*, 2017, **36**, 4519–4524.
47 M. L. Neidig, D. L. Clark and R. L. Martin, *Coord. Chem. Rev.*, 2013, **257**, 394–406.
48 K. C. Mullane, P. Hrobárik, T. Cheisson, B. C. Manor, P. J. Carroll and E. J. Schelter, *Inorg. Chem.*, 2019, **58**, 4152–4163.
49 E. A. Pedrick, P. Hrobárik, L. A. Seaman, G. Wu and T. W. Hayton, *Chem. Commun.*, 2016, **52**, 689–692.
50 L. A. Seaman, J. R. Walensky, G. Wu and T. W. Hayton, *Inorg. Chem.*, 2013, **52**, 3556–3564.
51 W. Wu, D. Rehe, P. Hrobárik, A. Y. Kornienko, T. J. Emge and J. G. Brennan, *Inorg. Chem.*, 2018, **57**, 14821–14833.
52 L. A. Seaman, P. Hrobárik, M. F. Schettini, S. Fortier, M. Kaupp and T. W. Hayton, *Angew. Chem.*, 2013, **52**, 3259–3263.

